



HAL
open science

Role of cilia activity and surrounding viscous fluid on properties of metachronal waves

Supravat Dey, Gladys Massiera, Estelle Pitard

► **To cite this version:**

Supravat Dey, Gladys Massiera, Estelle Pitard. Role of cilia activity and surrounding viscous fluid on properties of metachronal waves. 2023. hal-04279663

HAL Id: hal-04279663

<https://hal.science/hal-04279663>

Preprint submitted on 10 Nov 2023

HAL is a multi-disciplinary open access archive for the deposit and dissemination of scientific research documents, whether they are published or not. The documents may come from teaching and research institutions in France or abroad, or from public or private research centers.

L'archive ouverte pluridisciplinaire **HAL**, est destinée au dépôt et à la diffusion de documents scientifiques de niveau recherche, publiés ou non, émanant des établissements d'enseignement et de recherche français ou étrangers, des laboratoires publics ou privés.

Role of cilia activity and surrounding viscous fluid on properties of metachronal waves

Supravat Dey*

Department of Physics, SRM University - AP, Amaravati, Andhra Pradesh 522240

Gladys Massiera[†] and Estelle Pitard[‡]

*Laboratoire Charles Coulomb (L2C),
Université de Montpellier, CNRS,
34095 Montpellier, France*

Large groups of active cilia collectively beat in a fluid medium as metachronal waves, essential for some microorganisms motility and for flow generation in mucociliary clearance. Several models can predict the emergence of metachronal waves, but what controls the properties of metachronal waves is still unclear. Here, we investigate numerically a simple model for cilia in the presence of noise on regular lattices in one- and two-dimensions. We characterize the wave using spatial correlation and the frequency of collective beating. Our results clearly show that the viscosity of the fluid medium does not affect the wavelength; the activity of the cilia does. These numerical results are supported by a dimensional analysis, which is expected to be robust against the model for active force generation, unless surrounding fluid influences the cilia activity. Interestingly, enhancement of cilia activity increases the wavelength and decreases the beating frequency, keeping the wave velocity almost unchanged. These results might have significance in understanding paramecium locomotion and mucociliary clearance diseases.

The emergence of phase-travelling waves in dense arrays of active beating cilia, known as metachronal waves, is a complex multiscale physics problem [1–8] and is nonequilibrium because of the internal activity-driven movements of cilia [4]. The active beating of each cilium arises from the sliding of microtubules by thousands of molecular motors, and the subsequent interaction with the surrounding fluid medium. The coupling of a large number of these oscillators lead to synchronized dynamics over larger length scales. Illustrations are abundant in nature with ciliary living systems differing by cilia assembly geometry, cilia activity, or properties of the surrounding fluid. In respiratory tissues, the continuous cleaning of our lungs is provided by cilia beating waves that generate mucus flow [9, 10]. For certain microorganisms such as paramecium, synchronized beating of cilia help in their efficient locomotion [11]. The complexity of cilia active beating pattern and their interaction with each other through a complex environment makes it difficult to predict the emergent wave properties, despite recent theoretical and experimental advancements.

Models of cilia arrays [12–16], aim to identify the conditions required for such a coordinated state and to comprehend the physical parameters that govern the properties of the metachronal wave and the subsequent mucus transport. Several models have been proposed [12–14, 17], wherein the coupling is primarily described as a viscous hydrodynamic coupling. In these models, different types of active forces - from simple to complex, successfully generate continuous beating of a cilium. Numerical simulations enable to investigate the intricate structure of cilia by considering their beating as a filament bending wave [13, 18, 19]. Another approach is

to model cilia by actuated micron-sized beads called rotors [20–23] or rowers [12, 24, 25]. For a large group of cilia arranged in arrays, it has been shown that hydrodynamic coupling can lead to metachronal waves for various models of cilia [13, 15, 16].

Recently, the influence, on these collective behaviors, of several physical parameters such as noise [25, 26] and disorder in the arrangement and orientation of cilia has been investigated both numerically [25, 27, 28] and experimentally [28, 29], showing that spatial heterogeneity favors transport. Other important physical quantities that may play a role on the coordination are the activity and the dissipation, that will have opposite impacts on the metachronal waves emerging from cilia beating. Experimentally, a decrease in beating frequency with viscosity was found [30, 31], whereas the beating amplitude and the metachronal wavelength were found constant up to ≈ 50 times the viscosity of water [32, 33]. Theoretically, the mutual influence of activity and dissipation were almost not explored [34]. Here, our fundamental inquiry pertains to the interplay between cilia activity and fluid medium and its impact on the overall properties of metachronal waves.

To investigate this, we study the metachronal waves in the rower model of cilia in viscous fluid for one and two-dimensional regular lattices in the presence of thermal noise. In the rower model [12, 24, 25], the complex active beating of a cilium is simplified into the back and forth motion, along an axis, of a micron-sized bead immersed in a viscous fluid, thus ensuring a low Reynold's number regime. Such an oscillating motion is driven by two harmonic potential branches, corresponding to the stroke and anti-stroke of the cilia beating, with a geo-

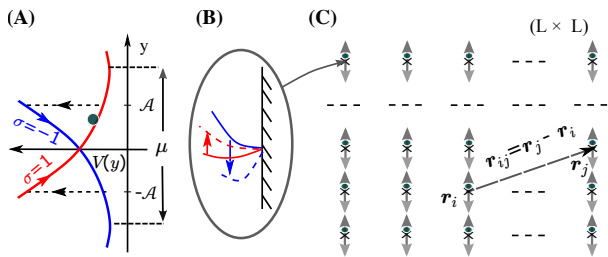


FIG. 1. Rower model of cilia [12]. (A) The motion of a micron-sized bead in a viscous medium under two harmonic potential branches, corresponding to $\sigma \pm 1$, represents the stroke and anti-stroke beating of a cilium. (B) The bead switches branches when it reaches terminal position $y = \pm A$. (C) Rowers beating along y -axis on two dimensional $L \times L$ regular lattices. Hydrodynamic interaction between rowers i and j is modelled by the Oseen coupling that depends on the separation vector \mathbf{r}_{ij} and viscosity of the medium.

metric switching mechanism. The bead moves downhill of a potential until it reaches one of the two terminal positions for which switching to the second branch occurs (Fig. 1A, B). This switching is like pumping energy to lift the bead on the upper side of the other potential at the terminal. At a given time, the bead can be found in one of these two states, the stroke and anti-stroke of the cilia beating, represented by a discrete $\sigma = \pm 1$. The driving force for a bead displacement y for a given σ can be written as

$$f(y, \sigma) = -\frac{dV(y, \sigma)}{dy} = -k(y - \sigma\mu/2), \quad (1)$$

where k is the force constant associated with the harmonic potentials, μ is the distance between minima of two potentials, and A is the beating amplitude. The supply of energies during each downhill motion in a harmonic potential, $kA^2/2$, and during each switch, the pumping energy $k\mu A$, keep the bead oscillating in the dissipating media. Therefore, for a given μ , the ‘activity’ of the bead depends on values of k and A . Because of its simplicity and ability to capture the two-stroke beating of cilia, the rower model has become a method of choice for theoretical and experimental studies of synchronization in ciliary systems [16, 29].

We consider a system of N rowers beating in the y direction in a viscous medium. Rowers are placed regularly in one- or two-dimensions (square) lattices (see Fig. 1C) at fixed positions \mathbf{r}_i (for $i = \{1, 2, 3, \dots, N\}$). The displacement, y_i , of a rower i is hydrodynamically coupled with the others and is given by

$$\frac{dy_i}{dt} = -\frac{f_i}{\gamma} + \sum_{j \neq i} O(i, j) f_j + \xi_i, \quad (2)$$

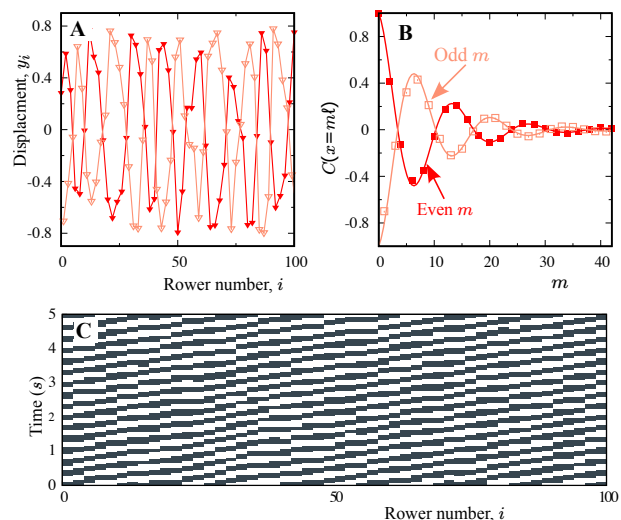


FIG. 2. Metachronal waves in 1d. A. Snapshot of displacements of the first 100 rowers. The displacement of even (odd) sites is plotted in light (dark) color. B. Correlation function $C(x=m\ell)$ between two rowers is plotted against separation distance x . C. Kymograph of the beating state σ , with white color (black) representing $\sigma=1$ ($\sigma=-1$). Parameters: $A = 0.8$, $\eta = 6$ mPa-s, and $N = 200$.

where $\gamma = 6\pi\eta a$ is the viscous drag coefficient for a bead with radius a moving in a fluid medium with viscosity η and $O(i, j)$ the coupling strength between rower i and j . In the far-field hydrodynamic coupling approximation, for which both the distance from the surface and the distance between two adjacent rowers (lattice spacing ℓ) are large compared to a , $O(i, j)$ is set by the Oseen tensor: $O(i, j) = \frac{1}{8\pi\eta r_{ij}} \left(1 + \left(\frac{y_{ij}}{r_{ij}}\right)^2\right)$, with $i \neq j$, and $\mathbf{r}_{ij} = \mathbf{r}_j - \mathbf{r}_i$, the separation vector between rowers i and j . The last term is due to the thermal noise, obeying the following delta-correlation: $\langle \xi(t) \rangle = 0$, $\langle \xi(t_1)\xi(t_2) \rangle = 2D\delta(t_1 - t_2)$. For simplicity, we assume no correlation between the noise acting on each of the rowers as in [25]. The noise strength or diffusivity is equal to $D = k_B T/\gamma$, k_B and T being the Boltzmann constant and the temperature. The displacement of a single isolated bead shows sustained oscillations with the frequency $\nu_0 = 1/(2\tau_d \log[(\mu + 2A)/(\mu - 2A)])$, where $\tau_d = \gamma/k$ is the relaxation time for the bead to reach equilibrium in a harmonic potential [24]. Such two coupled rowers beat collectively with antiphase synchronization [12]. For many rowers, the interplay between the activity of the rowers and coupling through the medium generates metachronal waves [12].

Simulation details - The Euler method with an integration step equal to $5 \times 10^{-3} s$ has been used to evolve the coupled dynamical equation (Eq. 2), starting from random initial values for $\{\sigma_i, y_i\}$. The open boundary condition is implemented. Parameters are chosen within the experimentally relevant range [24, 35], as

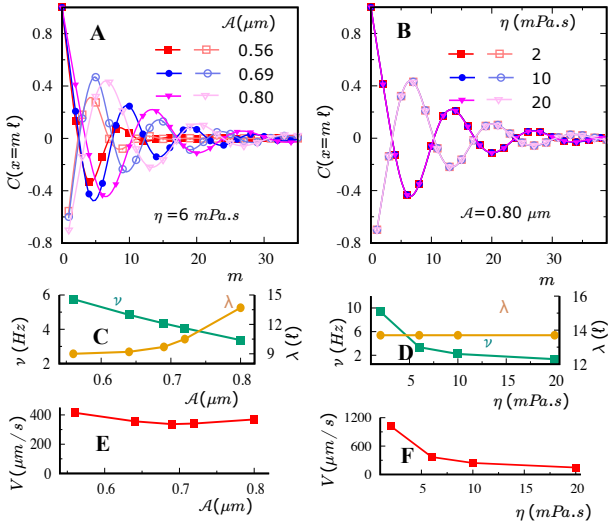


FIG. 3. Effect of viscosity and beating amplitude on metachronal waves in 1d ($N=200$). Correlation function $C(x=m\ell)$ as a function of the distance between rows, for three different \mathcal{A} values (for $\eta=6$ mPa.s) (A) and for three different η values (for $\mathcal{A}=0.80$ μm) (B). The wavelengths of metachronal waves λ are plotted against \mathcal{A} (C), and η (D), together with the corresponding beating frequency ν . Propagation velocity $V=\lambda\nu$ is plotted against \mathcal{A} (E), and η (F).

follows: $a=1.5$ μm , $\ell=8$ μm , $k=2.6$ $pN\cdot\mu\text{m}^{-1}$, $\mu=2$ μm , $\mathcal{A}=0.56 - 0.8$ μm , $\eta=2 - 20$ mPa.s, and $T=300$ K. Results presented here for large system sizes; $N=L=200$ (for 1d) and $N=L^2=1600$ (for 2d). Comparing results with smaller systems (not shown here), we confirm that the presented results have no system size dependence. *Results* - Fig. 2 shows the metachronal waves in the one-dimensional lattice. The beads' displacement against the rows' position for a given time displays two spatial waves that are visualized by connecting displacements y_i by lines for all rows at the even and odd lattice sites separately (Fig. 2A) in agreement with [12, 36]. This is a unique feature of the rower model, and arises due to a degree of anti-phase synchronization between two adjacent rows. The wave propagation is illustrated in Fig. 2C by the kymograph obtained for $\sigma_i(t)$. To characterize it, we compute the spatial correlation function between two rows as a function of their separation vector \mathbf{r} :

$$C(\mathbf{r}) = \frac{\sum_{ij} \langle \sigma_i(\mathbf{r}_i, t) \sigma_j(\mathbf{r}_j, t) \rangle \delta(\mathbf{r} - \mathbf{r}_{ij})}{\sum_{ij} \delta(\mathbf{r} - \mathbf{r}_{ij})}. \quad (3)$$

As the rowers are placed on a regular lattice with lattice spacing ℓ , the coordinates of \mathbf{r} are discrete and can be written as $(m\ell, n\ell)$ with $m, n \in \{0, 1, 2, \dots, L\}$. The measurement is done after a large equilibration time t_0 , where the system is assumed to reach a steady state. Brackets $\langle \cdot \rangle$ represent average over times and ensembles. An ensemble is the collection of 5000 sets of $\{\sigma_i(t)\}$ recorded every 2 seconds after $t_0=2500$ seconds.

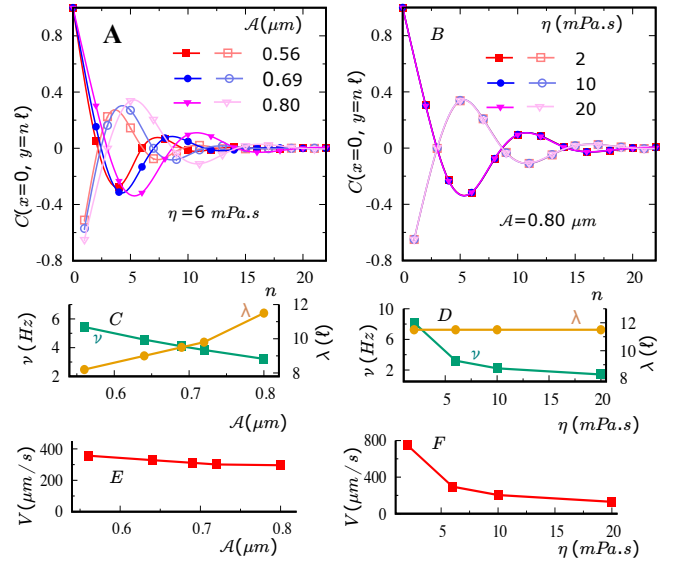


FIG. 4. Effect of viscosity and beating amplitude on metachronal waves in 2d ($N=L^2=1600$). Correlation function along beating direction $C(x=0, y=n\ell)$ as a function of the distance between rows, for three different values of \mathcal{A} (for $\eta=6$ mPa.s) (A) and for three different η values (for $\mathcal{A}=0.80$ μm) (B). The wavelengths of metachronal waves λ are plotted against \mathcal{A} (C), and η (D), together with the corresponding beating frequency ν . Propagation velocity $V=\lambda\nu$ is plotted as a function of \mathcal{A} (E), and η (F).

Fig. 2B shows the variation of $C(x) = C(x, y=0)$ in one dimension. For odd and even m values, two oscillating curves decay to zero as the distance between rows $x = m\ell$ increases. While the oscillations indicate the wave nature of the collective beating, the loss of correlations at larger x suggest a damping in the coordination on a characteristic length scale l_d . $C(x)$ can be fitted with the simple function $\pm e^{-x/l_d} \cos(2\pi x/\lambda)$, the $+$ ($-$) sign being for even (odd) m . This fit estimates the wavelength λ and decay length l_d . For Fig. 2, $\lambda \simeq 13.7\ell$ and $l_d \simeq 9.0\ell$. In a recent work, wavelength, and decay length were measured experimentally for metachronal waves on the human bronchial epithelium, and these two lengthscale values are comparable [37]. Our results are consistent with the experiment. The ensemble and spatial average of the beating frequency was computed: $\nu \simeq 3.4$ Hz and combined with λ to infer the metachronal wave velocity $V = \nu\lambda \simeq 370$ $\mu\text{m}\cdot\text{s}^{-1}$. These values are consistent with estimates that can be inferred directly from the slopes in the kymograph Fig. 2C.

We then investigate the effect of viscosity of the fluid medium and activity of the cilia on the metachronal waves quantities: λ , l_d , ν , and $V=\nu\lambda$, by computing $C(x)$ for various η and \mathcal{A} . The plot of $C(x)$ for different \mathcal{A} values shows that both the wavelength λ and the decay length l_d increase with \mathcal{A} (Fig. 3A and C), whereas the averaged beating frequency ν decreases with \mathcal{A} , keeping

the velocity of the wave V , almost constant (Fig. 3C and E). As ν_0 , the natural frequency of a single rowler, decreases with \mathcal{A} , the decrease of ν is expected. On the same line, increasing \mathcal{A} , which is a characteristic length of the problem, may naturally increase the length scale of the emerging collective dynamics. Thus the respective variation of ν and λ can be generally expected. What is remarkable though is that they compensate to result in an almost constant metachronal wave velocity. Interestingly, $C(x)$ does not depend on the values of η (see Fig. 3B), meaning λ and l_d are independent of η and implying that the spatial behavior of emergent waves does not depend on the fluid viscosity and are only determined by cilia activity parameters, in agreement with experimental observations [30, 33]. Below, we argued that such behavior is generally characteristic of a hydrodynamically coupled system. Finally, the frequency ν decreases as a function of η and so does V , as measured experimentally in [30, 33].

On a square lattice, we find that the metachronal wave propagates along the beating direction y whereas no wave is obtained in the perpendicular direction (Fig. 5), suggesting longitudinal waves. In Fig. 4A and B, we plot the correlation function along y -direction $C(0, y = n\ell)$ against n for various values of \mathcal{A} and η . Similar to 1d, two spatial waves can be seen for even and odd values of n for a given parameter set. For a fixed η , λ increases and ν decreases with \mathcal{A} , keeping the wave velocity V almost constant (Fig. 4C and E). On the contrary, λ remains constant and ν decreases with η , leading to a decrease in the velocity V with η (Fig. 4D and F). These results are consistent with the 1d results. We further note that although the qualitative behavior of metachronal waves in 1d and 2d are similar, the values of λ and V are relatively larger in 1d. This result raises interesting questions on the implications of the geometry of realistic ciliated tissues, which are mostly organized in 2d groups of cilia bundles.

In the direction perpendicular to beating, no oscillation is obtained (Fig. 5). $C(x, 0)$ either monotonically decays to zero as for large \mathcal{A} or shows a negative correlation for small $y = m\ell$ with odd m that eventually approaches zero for large m . For a given \mathcal{A} , $C(x, 0)$ does not depend on η (Fig. 5B), although odd and even m can follow different curves, reminiscent of $C(0, y)$. We compare the decay lengths of correlations along x and y directions $l_{d,x}$ and $l_{d,y}$. The decay length for the damped oscillations along y , $l_{d,y}$, can be estimated from the fitting method discussed above. The decay length $l_{d,x}$ is estimated from the exponential fit of the $C(x = m\ell, 0)$ for even m values. The ratio $l_{d,y}/l_{d,x}$ is plotted in the insets, one notes that $l_{d,y}/l_{d,x} \gtrsim 2$. For a fixed \mathcal{A} , it remains unchanged with η . However, for a given η , the ratio increases with cilia activity \mathcal{A} , which implies an enhancement of coherence along the beating direction

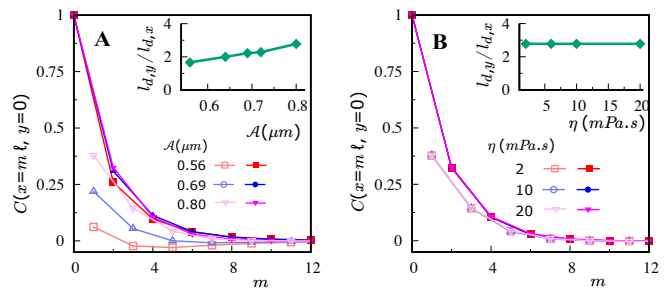


FIG. 5. Effect of viscosity and beating amplitude on correlations along the direction perpendicular to the beating direction $C(x=m\ell, y=0)$. A. $C(x=m\ell, y=0)$ for three different \mathcal{A} for a fixed $\eta=6$ mPa.s (A), and for three values of η for a given $\mathcal{A}=0.69\mu\text{m}$ (B).

compared the perpendicular one. This anisotropic response may be related to the anisotropy of the interaction strength. Indeed, considering the same r_{ij} value, $O(i, j)$ is two times larger along the y -axis than along the x -axis.

The fact that we obtain metachronal waves with spatial properties unaffected by viscosity has not been emphasized by previous studies, to our knowledge. Nevertheless, this remarkable numerical observation is robust on an order of magnitude of η obtained with both 1d and 2d simulations. To rationalize this result, one needs to look into the details of characteristic length, and timescales of the system set by the activity and the surrounding viscous medium. The relaxation time $\tau_d = 6\pi\eta a/k$ for the bead motion in the viscous medium under a harmonic driving potential, which also determines the natural frequency ν_0 of a single rowler, is a crucial timescale in our problem. In the rowler model, there are two lengths scales, the amplitude \mathcal{A} , and μ , the distance between the two branches of the potential (Fig. 1). Since we only vary \mathcal{A} , we chose it as the typical length scale. We note that our conclusion below, however, does not depend on the choice of the length scale. Multiplying both sides of Eq. 2 by τ_d/\mathcal{A} leads to an adimensional equation for the collective beating dynamics:

$$\frac{dy'_i}{dt'} = -f'_i - \sum_{i \neq j} \frac{3a}{4r_{ij}} (1 + (y_{ij}/r_{ij})^2) f'_j + \zeta_i(t'), \quad (4)$$

where t' and y' are dimensionless time $t' = t/\tau_d$ and displacement $y' = y/\mathcal{A}$, $f'_j = -(y'_j - \mu\sigma_j)/(2\mathcal{A})$ is the dimensionless force acting on rowler j , and $\langle \zeta(t'_1)\zeta(t'_2) \rangle = 2k_B T/(k\mathcal{A}^2)\delta(t'_1 - t'_2)$ is the adimensional noise correlation. As activity parameters \mathcal{A} , k , and μ are constant, Eq. 4 is η independent. The latter suggests that the spatial properties are independent of η . However, as τ_d is affected by η , it impacts the dynamical properties of the system. If any parameter \mathcal{A} , k , and μ are influenced by the medium, then our observation will break down.

We argue that the independence on fluid viscosity of

the spatial emergent properties is more generic to systems operating at low Reynold's numbers, irrespective of the model details. For systems at a low Reynold's number, both the viscous drag and hydrodynamic coupling between two objects are inversely proportional to η . The thermal noise strength D is also inversely proportional to η . As τ_d is inversely proportional to η , this also means that the normalization of Eq. 2 by τ_d will lead to the same conclusion. Therefore, one can get a similar adimensional equation as Eq. 4 for any model of active cilia coupled by a viscous fluid at low Reynolds numbers. Hence, the spatial properties of the emergent waves are expected to be independent of viscosity. If active beating is strongly dependent on the fluid rheology, then the active parameters of the rower model would depend on the viscosity, and this result would fail. Experimental results [31] seem to indicate though a very small dependence of cilia beating amplitude with the liquid medium. We note that additional sources of deviation from this result could be the viscoelastic nature of the fluid or a non-thermal noise, which we have not addressed in this paper. Finally, although this simple dimensional analysis cannot predict the occurrence or nature of emergent behavior, it is powerful in predicting that the wavelength or other spatial properties will be viscosity independent in general.

In conclusion, we have presented simple generic results about complex dynamics of hydrodynamically coupled model cilia. Using a very simple rower model of coupled oscillators, we have focused our study on the influence of activity and dissipation on the spatial and temporal synchronization properties of cilia assemblies. Enhancement of cilia activity increases the wavelength and beating period, keeping the wave velocity almost unchanged. On the other hand, viscosity does not affect spatial patterns characterizing metachronal waves such as wavelength or correlation lengths. On the contrary, the beating frequency and the wave velocity indeed decrease with viscosity. The deviation from such a behaviour may indicate the influence of additional properties of the medium not taken into account in the coupling description of the current model and could also be a signature of viscoelasticity or elasticity of the tissue itself. This could pave the way to the study of the emergence of specific functions of cilia in pathological contexts for example [23].

* supravat.dey@gmail.com

† gladys.massiera@umontpellier.fr

‡ estelle.pitard@umontpellier.fr

- [1] J. Gray, *Ciliary movement* (Cambridge University Press, 1928).
- [2] M. A. Sleight, *The Biology of Cilia and Flagella* (Pergamon Press, 1962).
- [3] J. Blake, *Journal of Fluid Mechanics* **55**, 1 (1972).

- [4] C. Battle, C. P. Broedersz, N. Fakhri, V. F. Geyer, J. Howard, C. F. Schmidt, and F. C. MacKintosh, *Science* **352**, 604 (2016).
- [5] W. Gilpin, M. S. Bull, and M. Prakash, *Nature Reviews Physics* **2**, 74 (2020).
- [6] E. Milana, R. Zhang, M. R. Vetrano, S. Peerlinck, M. D. Volder, P. R. Onck, D. Reynaerts, and B. Gorissen, *Science Advances* **6**, eabd2508 (2020).
- [7] D. R. Brumley, M. Polin, T. J. Pedley, and R. E. Goldstein, *Journal of The Royal Society Interface* **12**, 20141358 (2015).
- [8] R. Zhang, J. den Toonder, and P. R. Onck, *Physics of Fluids* **33**, 092009 (2021).
- [9] A. Wanner, M. Salathé, and T. G. O'Riordan, *American journal of respiratory and critical care medicine* **154**, 1868 (1996).
- [10] D. Smith, E. Gaffney, and J. Blake, *Respiratory physiology and Neurobiology* **163** (2008).
- [11] E. Lauga, *The fluid dynamics of cell motility*, Vol. 62 (Cambridge University Press, 2020).
- [12] M. C. Lagomarsino, P. Jona, and B. Bassetti, *Physical Review E* **68**, 021908 (2003).
- [13] J. Elgeti and G. Gompper, *Proc. Natl. Acad. Sci. USA* **110**, 4470 (2013).
- [14] R. Golestanian, J. M. Yeomans, and N. Uchida, *Soft Matter* **7**, 3074 (2011).
- [15] N. Uchida, R. Golestanian, and R. R. Bennett, *Journal of the Physical Society of Japan* **86**, 101007 (2017).
- [16] B. Chakrabarti, S. Fürthauer, and M. J. Shelley, *Proceedings of the National Academy of Sciences* **119**, e2113539119 (2022).
- [17] T. Niedermayer, B. Eckhardt, and P. Lenz, *Chaos: An Interdisciplinary Journal of Nonlinear Science* **18**, 037128 (2008).
- [18] M. Leoni and T. B. Liverpool, *Phys. Rev. E* **85**, 040901 (2012).
- [19] B. Guirao and J. F. Joanny, *Biophysical Journal* **92**, 1900 (2007).
- [20] N. Uchida and R. Golestanian, *Phys. Rev. Lett.* **106**, 058104 (2011).
- [21] D. R. Brumley, N. Bruot, J. Kotar, R. E. Goldstein, P. Cicuta, and M. Polin, *Phys. Rev. Fluids* **1**, 081201 (2016).
- [22] F. Meng, R. R. Bennett, N. Uchida, and R. Golestanian, *Proceedings of the National Academy of Sciences* **118**, e2102828118 (2021).
- [23] A. V. Kanale, F. Ling, H. Guo, S. Fürthauer, and E. Kanso, *Proceedings of the National Academy of Sciences* **119**, e2214413119 (2022).
- [24] J. Kotar, M. Leoni, B. Bassetti, M. C. Lagomarsino, and P. Cicuta, *Proceedings of the National Academy of Sciences* **107**, 7669 (2010).
- [25] E. Hamilton and P. Cicuta, *PLOS ONE* **16**, 1 (2021).
- [26] A. Solovev and B. M. Friedrich, *New Journal of Physics* **24**, 013015 (2022).
- [27] S. Dey, G. Massiera, and E. Pitard, *Phys. Rev. E* **97**, 012403 (2018).
- [28] G. R. Ramirez-San Juan, A. J. Mathijssen, M. He, L. Jan, W. Marshall, and M. Prakash, *Nature physics* **16**, 958 (2020).
- [29] N. Pellicciotta, E. Hamilton, J. Kotar, M. Faucourt, N. Delgehyr, N. Spassky, and P. Cicuta, *Proceedings of the National Academy of Sciences* **117**, 8315 (2020).

- [30] H. Machemer, *J. Exp. Biol.* , 57 (1972).
- [31] N. T. Johnson, M. Villalon, F. H. Royce, R. Hard, and P. Verdugo, *AM REV RESPIR DIS* **144**, 1091 (1991).
- [32] K. Kikuchi, T. Haga, K. Numayama-Tsuruta, H. Ueno, and T. Ishikawa, *Annals of biomedical engineering* **45**, 1048 (2017).
- [33] L. Gheber, A. Korngreen, and Z. Priel, *Cell Motility* **39**, 9 (1998).
- [34] L. Gheber and Z. Priel, *Cell Motility* **16**, 167 (1990).
- [35] D. R. Brumley, M. Polin, T. J. Pedley, and R. E. Goldstein, *Phys. Rev. Lett.* **109**, 268102 (2012).
- [36] C. Wollin and H. Stark, *Eur. Phys. J. E* **34**, 42 (2011).
- [37] O. Mesdjian, C. Wang, S. Gsell, U. D’Ortona, J. Favier, A. Viallat, and E. Loiseau, *Phys. Rev. Lett.* **129**, 038101 (2022).